Technical Report No. 32-619

Correlation of Launch-Vehicle Wind-Tunnel Aerodynamic Noise With Spacecraft Flight Vibration Data (Revision No. 1)

Robert A. Schiffer

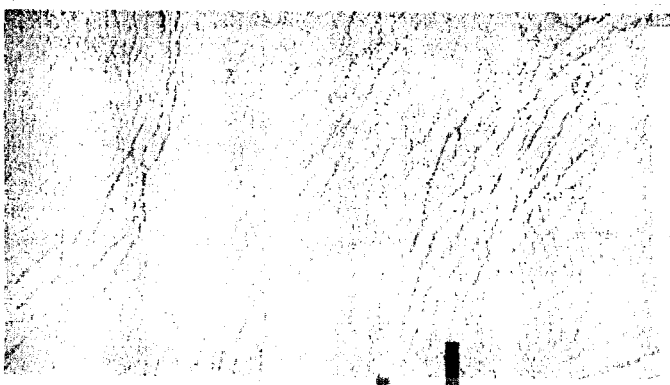

jpl

JET PROPULSION LABORATORY
CALIFORNIA INSTITUTE OF TECHNOLOGY
PASADENA, CALIFORNIA

September 15, 1964

Technical Report No. 32-619

Correlation of Launch-Vehicle Wind-Tunnel Aerodynamic Noise With Spacecraft Flight Vibration Data (Revision No. 1)

Robert A. Schiffer

W. S. Shipley, *Chief*
Program Engineering

JET PROPULSION LABORATORY
CALIFORNIA INSTITUTE OF TECHNOLOGY
PASADENA, CALIFORNIA

September 15, 1964

Prepared Under Contract No. NAS 7-100
National Aeronautics & Space Administration

CONTENTS

TABLES

FIGURES

PREFACE

Various portions of this Report were prepared for presentation at the 67th meeting of the Acoustical Society of America, held in New York City, May 1964.

ABSTRACT

3315B

It has been observed that the maximum vibration levels experienced by a launch vehicle occur in the regions of q_{max} and transonic flight. Flight vibration data from *Ranger* spacecraft launches 1 through 6 have been correlated with available wind-tunnel fluctuating pressure data at transonic speeds in order to develop a technique for vibration prediction for types of vehicles that have not previously been flown. Statistical analysis of the wide-band vibration data suggests a linear correlation with the wind-tunnel wide-band fluctuating pressure data. Correlation is also explored between the average vibration response spectra calculated by using the empirical method suggested by P. Franken and the 50-percentile log-normal acceleration confidence level obtained by spectral analysis of the flight data.

I. INTRODUCTION

In general, vibration test specifications for spacecraft are based on conservative estimates of the expected flight environment. In-flight vibration data then become invaluable for refining these estimates, thereby making them more representative of actual flight. In addition, these data provide a basis for the development of techniques for predicting the vibration environments for similar launch systems.

It has been observed that the maximum vibration levels experienced by a launch vehicle occur in the regions of q_{max} and transonic flight. These strong vibrations are generated in part by the unsteady aerodynamic loads associated with transonic buffeting. Fluctuating pressures associated with transonic buffeting have been investigated for a large number of launch vehicle configurations, as reported in Ref. 1–5.

The present investigation is intended to show that a favorable correlation has been observed between the transonic wind-tunnel fluctuating pressure data obtained for the *Ranger* configuration *Atlas-Agena* launch vehicle (Fig. 1) and the in-flight vibration data recorded for *Ranger* launches 1 through 6.

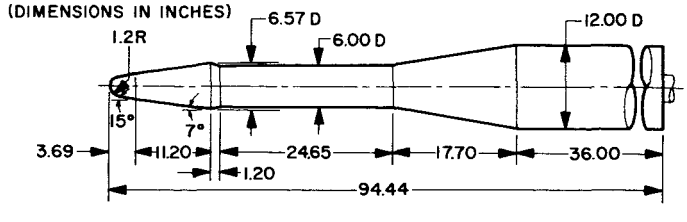

Fig. 1. Wind-tunnel model of the *Ranger* configuration *Atlas-Agena* vehicle

II. FLUCTUATING PRESSURE DATA

A series of wind-tunnel tests was conducted at the Ames Research Center of the National Aeronautics and Space Administration to investigate the fluctuating pressures at transonic speeds along the surface of a 1/10-scale model of the *Ranger* configuration *Atlas–Agena* launch vehicle. The results of these tests are reported in Ref. 3. The test model was instrumented with a series of strain-gage-type pressure transducers located along the longitudinal axis of the model and at various peripheral angles. A detailed description of the data-acquisition instrumentation is presented in Ref. 1. Runs were made at selected incremental transonic Mach numbers from 0.70 to 1.17, for angles of attack of 0, 4, and 8 deg. Since the significant flow disturbances occur in the vicinity of the spacecraft shroud boattail at zero angle of attack, the pressure fluctuation data in this region only were considered for correlation with the vibration data. Figure 2 summarizes the pertinent fluctuating pressure data for the shroud boattail region.

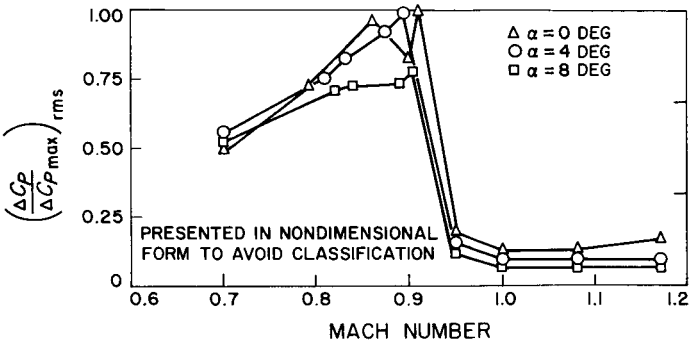

Fig. 2. $\Delta C_{p\ rms}$ vs Mach number for the *Ranger* configuration *Atlas-Agena* vehicle model

III. VIBRATION DATA

The vibration data recorded for *Ranger 1* through *4* have been reduced to one form of wide-band acceleration-time history plots. In each case the accelerometer was mounted to the transition section between the *Ranger* spacecraft and the *Agena* vehicle. The accelerometer location and mounting configuration are shown in Fig. 3. The rms acceleration-time histories for transonic flight are presented in Fig. 4.

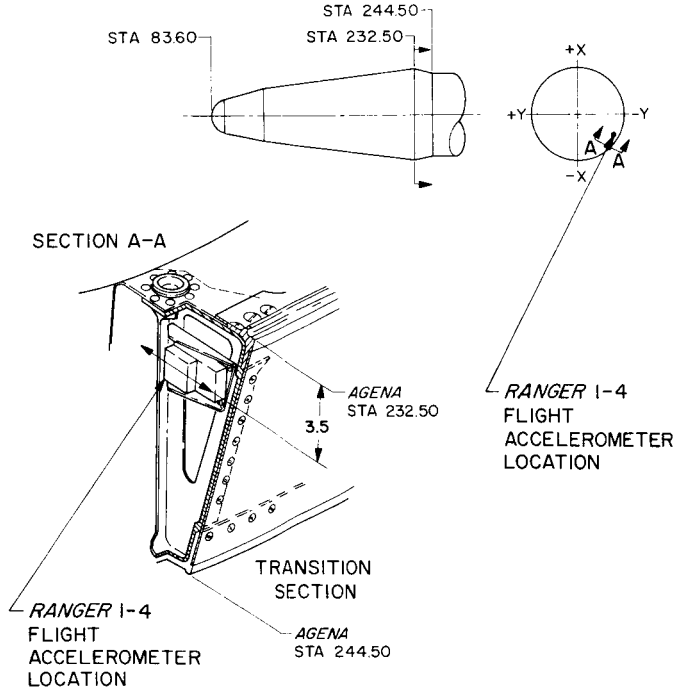

Fig. 3. Accelerometer location and mounting configuration

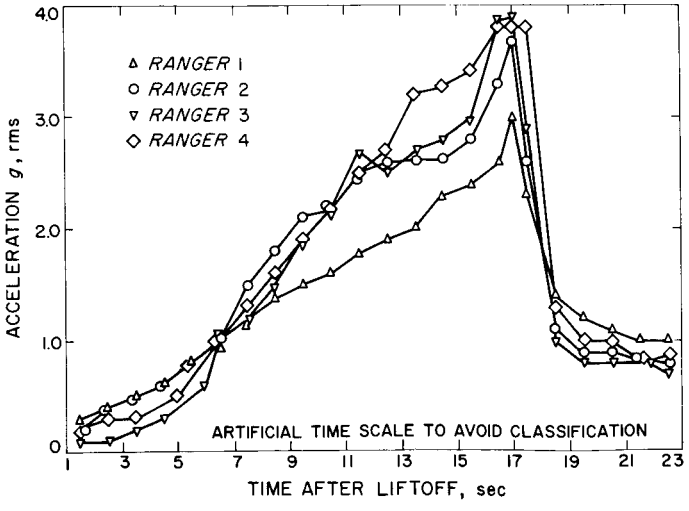

Fig. 4. Acceleration-time history for *Ranger* spacecraft launches

IV. DATA CORRELATION

The wind-tunnel test data were reported in non-dimensional form as

$$\Delta C_{p\,\mathrm{rms}} = \frac{\Delta P_{\mathrm{rms}}}{q}$$

For each wind-tunnel test Mach number, the time of flight and dynamic pressure were obtained from the actual *Ranger* launch trajectory-time histories. Corresponding rms accelerations were obtained from Fig. 4. The values for P_{rms} were determined as indicated in Table 1, where $\Delta P_{\mathrm{rms}} = \Delta C_{p\,\mathrm{rms}} \times q_\infty$. The equivalent acoustic sound pressure levels in decibels were then computed, using the relationship

$$SPL = 20 \log_{10} \frac{\Delta P_{\mathrm{rms}}}{P_{\mathrm{ref}}}$$

The results in Table 1 are illustrated in Fig. 5, which shows the relationship between the fluctuating pressures measured at the boattail of the launch vehicle shroud and the recorded wide-band vibration levels. A statistical analysis of the data was performed to determine whether a linear correlation exists between the fluctuating pressure and vibration data. A least-squares line was computed and a correlation coefficient of 0.93 obtained, considering 32 data points.

As reported in Ref. 3, the wide-band fluctuating pressure data were reduced to power spectral density (PSD) plots using a constant-bandwidth spectral analyzer. The results indicate the PSD to be essentially flat to 500 cps, which was the limit of the analysis. In applying these data to the full-scale vehicle, it was assumed that Strouhal-number and fluctuating pressure coefficient scaling are applicable. The pertinent PSD and frequency scaling parameters are developed in the Appendix. It was further

Table 1. Determination of P_{rms} and *SPL*

Mach	$\left(\frac{\Delta C_p}{\Delta C_{p\,\max}}\right)_{\mathrm{rms}}$[a]	T sec	ΔP_{rms} lb/ft²	*SPL*[b] db
0.70	0.500	7.5	5.85	142.3
0.79	0.734	11.0	10.55	147.5
0.86	0.966	14.0	15.95	151.1
0.90	0.833	15.0	14.50	150.2
0.91	1.000	15.5	18.30	152.2
1.00	0.133	18.5	2.68	135.6
1.08	0.133	20.5	2.84	136.1
1.17	0.167	24.0	3.80	138.6

[a]Normalized to the maximum value
[b]Ref: 0.0002 dynes/cm²

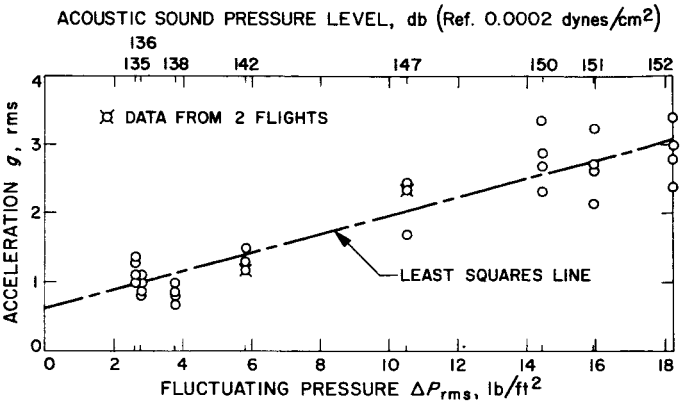

Fig. 5. Correlation of launch vehicle fluctuating pressure and *Ranger* spacecraft vibration

assumed that the PSD for the fluctuating pressures is flat throughout the frequency range of interest. Reynolds-number effects were neglected. Based on these assumptions, the maximum wide-band *SPL* of 152.2 db from Table 1 was adjusted to the full-scale vehicle level of 160.4 db and converted to ⅓-octave bands (Table 2) using the following relationship:

$$SPL_{1/3} = SPL_{wb} - 10 \log_{10} \frac{\Delta f_{wb}}{\Delta f_{1/3}}$$

The average spacecraft transonic-vibration response spectra were estimated (Table 3), using the empirical procedure suggested by Franken (Ref. 6) as illustrated in Fig. 6, where

$$20 \log g = SPL - 20 \log w + TF$$

The results in Table 3 were converted to 1 cps bandwidth and are illustrated in Fig. 7, which compares the estimated acceleration with the 50-percentile log-normal acceleration confidence levels measured during transonic

Table 2. Conversion of *SPL* to 1/3-octave bands

$f_{1/3}$[a]	$\Delta f_{1/3}$	SPL_{wb}	$SPL_{1/3}$
200	46	160.4	157.0
400	92	160.4	160.0
630	146	160.4	162.0
800	183	160.4	163.0
1000	230	160.4	164.0
1250	290	160.4	165.0
1600	370	160.4	167.0

[a]Based on standard 1/3-octave bandpass filters

flight (Ref. 7). It should be noted that the flight-data reduction was performed using 2-sec time samples during which the flow field changed significantly, whereas the wind-tunnel fluctuating pressure data were obtained under stationary flow conditions. This may account for some of the discrepancy between the estimated and flight vibration levels.

Table 3. Estimated transonic vibration response spectra

f	Δf	SPL	TF[a]	$\log_{10} g$	$g^2/\Delta f$
200	46	157.0	−137.5	0.050	0.028
400	92	160.0	−131.0	0.525	0.111
630	146	162.0	−125.0	0.925	0.486
800	183	163.0	−122.0	1.125	0.974
1000	230	164.0	−121.0	1.175	0.980
1250	290	165.0	−121.5	1.25	1.09
1600	370	166.3	−122.0	1.29	1.06

[a]See Fig. 6.

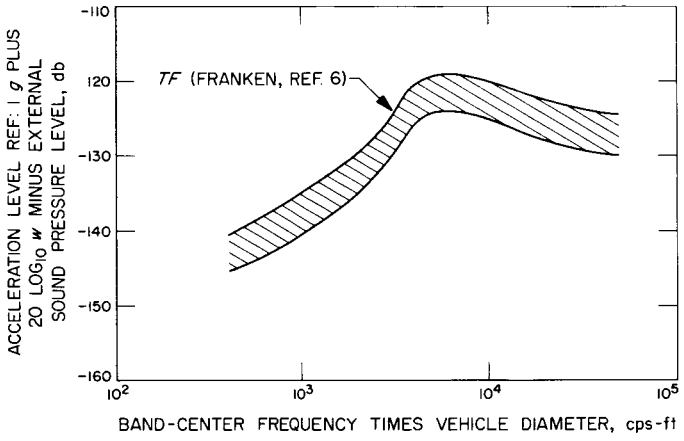

Fig. 6. Generalized relation between external noise and radial skin vibration

The transonic vibration spectra for *Ranger 6* are also shown in Fig. 7 to demonstrate the effect of altering the location of the vibration transducer. For this flight, the accelerometer was repositioned within 3 in. of the original location, shown in Fig. 3.

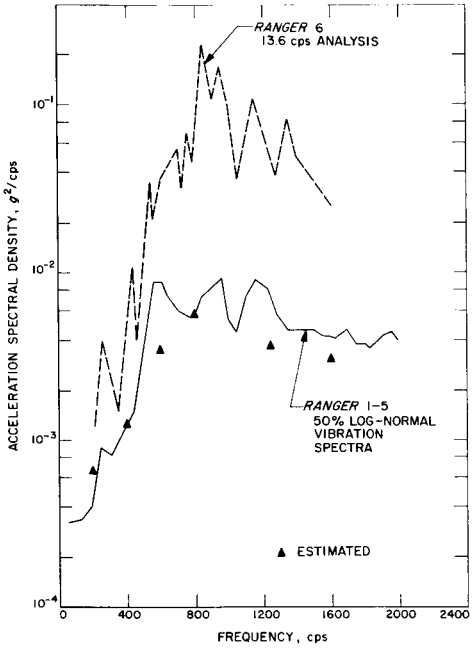

Fig. 7. Comparison of estimated and measured transonic vibration

V. ACOUSTIC SUSCEPTIBILITY TESTS

To study the effects of the repositioning of the accelerometer on *Ranger 6*, a series of acoustic susceptibility tests was performed in the 12-ft acoustic reverberation chamber at the Jet Propulsion Laboratory. An *Agena* forward structure was supported on rubber isolator pads on the chamber floor. Spacecraft adaptor sections having *Ranger 4* and *Ranger 6* flight accelerometer mounting configurations were attached and subjected to a 142-db acoustic field. For each configuration, the forward end of the adaptor was covered with 1-in. plywood board. The acoustic susceptance at the flight accelerometer location for each configuration was determined by calculating the ratio of the measured vibration excited by the acoustic field to the sound pressure level measured at the external microphone nearest the accelerometer. The ratio of the acoustic susceptance spectra for *Ranger 4* to *Ranger 6* is presented in Fig. 8.

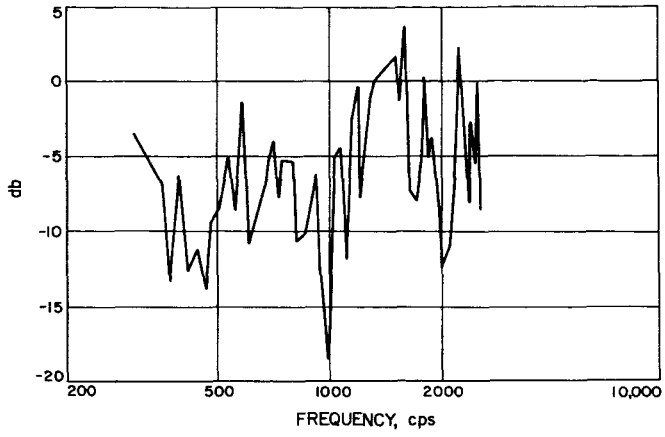

Fig. 8. Ratio of acoustic susceptance, *Ranger 4* to *Ranger 6*

VI. CONCLUSIONS

The existence of a good correlation has been demonstrated between the recorded in-flight wide-band vibration data and the measured wind-tunnel fluctuating pressure data for the *Ranger* configuration *Atlas–Agena* launch vehicle at transonic speeds. This correlation suggests that wide-band vibration levels can possibly be predicted for accelerometers mounted on similar types of structures for a variety of launch vehicles.

However, the extremely localized nature of the validity of the flight vibration measurements near the vehicle skin must be recognized. The nature of the flight vibration data from *Ranger 6* and the results of the acoustic susceptibility tests at the Jet Propulsion Laboratory give evidence of the necessity for first measuring the structural acoustic susceptance and then using that data and the estimates of the sound pressure spectrum to predict vibration levels. The predicted wide-band levels and spectral scale based on previous flight data from similar vehicles, wind-tunnel ΔC_p data, and acoustic susceptance data may provide a somewhat realistic basis for vibration test definition for types of vehicles which have not previously been flown.

NOMENCLATURE

C_p	pressure coefficient, $(P - P_\infty)/q_\infty$
ΔC_p	change in pressure coefficient, $(C_{p1} - C_{p2})$
D	vehicle diameter, ft
f	frequency, cps
fs	full-scale vehicle
m	model
M_∞	free-stream Mach number
P	local static pressure, lb/ft^2
q	dynamic pressure, lb/ft^2
S	power spectral density, psf^2/cps
SPL	sound pressure level, db
TF	acoustic transfer function
V	velocity, ft/sec
w	shroud unit skin weight, lb/ft^2
α	angle of attack, deg
γ	ratio of specific heats
σ	pressure fluctuation, $(P - P_\infty)_{rms}$

Subscripts

$1/3$	one-third octave band
∞	free stream
rms	root mean square
wb	wide band

REFERENCES

1. Coe, C. F., *Steady and Fluctuating Pressures at Transonic Speeds on Two Space Vehicle Payload Shapes,* NASA TMX-503, National Aeronautics and Space Administration, Washington, D. C., 1961. CONFIDENTIAL.
2. Coe, C. F., *The Effects of Some Variations in Launch Vehicle Nose Shape on Steady and Fluctuating Pressures at Transonic Speeds,* NASA TMX-646, National Aeronautics and Space Administration, Washington, D. C., 1962. CONFIDENTIAL.
3. Coe, C. F. and J. B. Nute, *Steady and Fluctuating Pressures at Transonic Speeds on Hammerhead Launch Vehicles,* NASA TMX-778, National Aeronautics and Space Administration, Washington, D. C., 1962. CONFIDENTIAL.
4. Coe, C. F. and A. J. Kaskey, *The Effects of Nose Bluntness on the Pressure Fluctuations Measured on 15° and 20° Cone-Cylinders at Transonic Speeds,* NASA TMX-779, National Aeronautics and Space Administration, Washington, D. C., 1963. CONFIDENTIAL.
5. Cole, H. A., Jr., *Dynamic Response of Hammerhead Launch Vehicles to Transonic Buffeting,* NASA TMD-1982, National Aeronautics and Space Administration, Washington, D. C., 1963.
6. Franken, P. A., "Sound Induced Vibrations of Cylindrical Vehicles," *Journal of the Acoustical Society of America,* Vol. 34, No. 4, April 1962.
7. Bolt, Beranek and Newman, Inc., *Noise and Noise-induced Structural Vibration of the Ranger Spacecraft,* Report No. 1038, Bolt, Beranek and Newman, Inc., Los Angeles, Calif., 1963.

APPENDIX

Scaling of Wind-Tunnel Data

Strouhal number

$$\frac{fm\,Dm}{Vm} = \frac{f_{fs}\,D_{fs}}{V_{fs}} \qquad \text{(A-1)}$$

Pressure coefficient

$$\Delta C_p = \frac{\sigma_m}{q_m} = \frac{\sigma_{fs}}{q_{fs}} \qquad \text{(A-2)}$$

The power spectral density of the pressure fluctuation is defined as

$$S = \frac{\sigma^2}{\Delta f}$$

or

$$\sigma = (S\Delta f)^{1/2}$$

and

$$\Delta C_p = \frac{(S\Delta f)^{1/2}}{q}$$

From Eq. A-2

$$\frac{[S_m \Delta f_m]^{1/2}}{q_m} = \frac{[S_{fs}\Delta f_{fs}]^{1/2}}{q_{fs}}$$

$$S_{fs} = \left(\frac{q_{fs}}{q_m}\right)^2 \left(\frac{\Delta f_m}{\Delta f_{fs}}\right) \times S_m$$

substituting Eq. A-1, the full-scale power spectral density is expressed as

$$S_f = \left(\frac{q_{fs}}{q_m}\right)^2 \left(\frac{V_m}{V_{fs}}\right)\left(\frac{D_{fs}}{D_m}\right) \times S_m$$

The frequency is scaled by virtue of Eq. A-1, resulting in

$$f_{fs} = \left(\frac{V_{fs}}{V_m}\right)\left(\frac{D_m}{D_{fs}}\right) \times f_m$$